doi:10.3772/j.issn.1006-6748.2022.02.001

Deep learning based Doppler frequency offset estimation for 5G-NR downlink in HSR scenario①

YANG Lihua(杨丽花)②*, WANG Zenghao*, ZHANG Jie*, JIANG Ting**
(*College of Communication and Information Engineering, Nanjing University of Posts and Telecommunications, Nanjing 210003, P.R.China)
(**College of Electronic and Information Engineering, Nanjing University of Aeronautics and Astronautics, Nanjing 210016, P.R.China)

Abstract

In the fifth-generation new radio (5G-NR) high-speed railway (HSR) downlink, a deep learning (DL) based Doppler frequency offset (DFO) estimation scheme is proposed by using the back propagation neural network (BPNN). The proposed method mainly includes pre-training, training, and estimation phases, where the pre-training and training belong to the off-line stage, and the estimation is the online stage. To reduce the performance loss caused by the random initialization, the pre-training method is employed to acquire a desirable initialization, which is used as the initial parameters of the training phase. Moreover, the initial DFO estimation is used as input along with the received pilots to further improve the estimation accuracy. Different from the training phase, the initial DFO estimation in pre-training phase is obtained by the data and pilot symbols. Simulation results show that the mean squared error (MSE) performance of the proposed method is better than those of the available algorithms, and it has acceptable computational complexity.

Key words: fifth-generation new radio (5G-NR), high-speed railway (HSR), deep learning (DL), back propagation neural network (BPNN), Doppler frequency offset (DFO) estimation

0 Introduction

With the rapid development of high-speed railway (HSR), the HSR wireless communication has attracted more and more attentions around the world[1-2], and HSR has been used as one of the important usage scenarios of the fifth-generation new radio (5G-NR) communication network. In the 5G-NR system, the HSR is expected to achieve a moving speed of up to 500 km/h. However, the high mobility will significantly limit the coverage area and transmission rate, and most current wireless communication systems are designed for the low or medium mobility scenarios. Therefore, it is necessary to design a reliable and efficient communication system for 5G-NR HSR (up to 500 km/h) scenario[3-5].

In 5G-NR HSR scenario, the Doppler shift will become large due to the increase in vehicle speed and the use of high carrier frequency bands. The large Doppler shift will cause more serious inter-carrier interference, which seriously affects the performance of the HSR communication system[6-7]. Therefore, the anti-Doppler frequency shift technology is very important in 5G-NR HSR environment, where the Doppler frequency offset (DFO) estimation and compensation technology is the basis.

Although many DFO estimation methods in high-speed mobile scenarios have been developed, most of them are carried out for HSR scenarios under 4G-LTE systems[8-11]. Due to the increase in vehicle speed and the use of high carrier frequencies, the Doppler frequency shift of 5G-NR HSR scenario is larger than that of 4G-LTE HSR scenario, so the existing estimation schemes in 4G-LTE HSR scenario cannot be directly used for 5G-NR HSR scenario.

Currently, there have been a few DFO estimation methods for the 5G-NR HSR scenario[6,12-13], where the Ref.[6] gave a DFO estimation and compensation algorithm based on position and pre-compensation for the millimeter-wave HSR system, which calculated the Doppler shift according to the position and speed of the

① Supported by the National Science Foundation Program of Jiangsu Province (No. BK20191378), the National Science Research Project of Jiangsu Higher Education Institutions (No. 18KJB510034), the 11th Batch of China Postdoctoral Science Fund Special Funding Project (No. 2018T110530), and the National Natural Science Foundation of China (No. 61771255).

② To whom correspondence should be addressed. E-mail: yanglh@njupt.edu.cn.

Received on May 27, 2021

train. However, it relies on high-precision positioning, while the positioning error cannot be avoided in practice. In Ref. [12], a DFO elimination method was presented for a millimeter-wave HSR mobile communication system, where the frequency offsets of the received signals of the head and the tail antennas located on the train are assumed to be the same, but have opposite direction. By multiplying the received signals from head and tail antennas, it can eliminate the Doppler shift. However, when the train passes the base station, the DFO will rapidly change, and the time of the head-to-tail antennas passing through the base station is different, so its performance will be deteriorated when the train is handed over. In Ref. [13], a pilot-based maximum likelihood DFO estimation method was given, which estimates the DFO by segmenting the pilot and solving the maximum likelihood function, but it requires a large computational complexity to obtain high estimation accuracy. To meet the requirements of pilot special segmentation, the scheme in Ref. [13] has a strict limit on the length of the pilot symbols, so it is not suitable for systems where the pilot structure has been determined.

In addition, artificial intelligence, especially deep learning (DL), has been applied into the fields of computer vision, natural language processing, speech recognition, etc.[14]. Moreover, the DL is also applied to the wireless communication systems, such as channel estimation, signal detection and channel decoding, etc. In the previous work, a DL-based DFO estimation method has been presented in Ref. [15], which is mainly divided into two stages, off-line training and online estimation. In the previous work, the training samples are constructed only by the received pilot signals, and then the training samples are employed to train the back propagation neural network (BPNN) in an off-line manner. Based on the trained network, the DFO can be estimated. Although the algorithm in Ref. [15] has a better estimation accuracy than the existing schemes, its performance still needs to be further improved.

Currently, the existing DL-based algorithms are mainly carried out from two aspects, one is to obtain better estimation results by using different neural networks[16-17], and the other is to obtain good results from designing the input values of the network[18-19]. To improve the performance of DFO estimation, a novel DL-based method is proposed from designing the initial value or input value of the network in the paper, which belongs to the second aspect.

The proposed DL-based method mainly contains three phases, i. e., pre-training, training and estimation stages. In the pre-training phase, the training samples are constructed by the received signal and initial DFO estimation, where the initial DFO is estimated by the data and pilot signals. In the training phase, only the received pilots and initial DFO estimation is used to train the BPNN, and the initial DFO estimation is obtained by the pilots. Due to the pre-training and initial DFO estimation, the performance of proposed method is greatly improved.

The rest of this paper is organized as follows. Section 1 introduces the system model. Section 2 presents the proposed method in detail. The simulation results and conclusions are given in Section 3 and Section 4 respectively.

1 Signal model

In a 5G-NR downlink single input single output-orthogonal frequency division multiple access (SISO-OFDMA) system, assume that the nth transmitted time domain signal during the mth OFDMA symbol in the ith subframe is $s_i(m, n)$. Since the Ricean-fading channel is often employed as the HSR channel[20-22], the discrete-time multipath Ricean-fading channel during the mth OFDMA symbol in the ith subframe is given as[23]

$$h_i(m,n) = c_i \exp[j2\pi\varepsilon_{i,m}(mN_D - N + n)/N] + \sum_{l_p=0}^{L_p-1} \alpha_{i,l_p}(m, n)\delta(m, n - \tau_{l_p}) \tag{1}$$

where c_i is the line of sight (LoS) path of Ricean-fading channel, $\alpha_{i,l_p}(m, n)$, $l_p(l_p = 0, \cdots)$, and $L_p - 1$ are the scattered paths, which follow the Rayleigh distribution, L_p is the number of the paths of the multipath Ricean-fading channel. $\varepsilon_{i,m}$ is the normalized DFO by the subcarrier spacing, τ_{l_p} is the l_pth time delay normalized by the sampling time of the path. $N_D = N + N_{cp}$, N_{cp} is the length of the cyclic prefix (CP), and N is the length of fast Fourier transform (FFT).

Assume that the timing synchronization is perfect at the receiver, and the nth received signal at the sample time during mth OFDMA symbol in the ith subframe is

$$r_i(m, n) = c_i s_i(m, n) e^{\frac{j2\pi\varepsilon_{i,m}(mN_D-N+n)}{N}} + w_i(m, n) + \sum_{l_p=0}^{L_p-1} \alpha_{i,l_p}(m, n) s_i(m, n - \tau_{l_p}) \tag{2}$$

where $w_i(m, n)$ is the additive white Gaussian noise (AWGN) with the covariance σ_w^2.

Since the change of frequency offset during one

OFDMA symbol is relatively small, the frequency offset in one subframe can be regarded as a constant. Moreover, the processing of the DFO estimation in each subframe is the same. Therefore, the subscript ith and superscript mth can be omitted to derive conveniently in the following.

2 Proposed DFO estimation method

In the section, the architecture of BPNN is given first, and then the proposed method will be introduced in detail.

2.1 BPNN

In the field of DL, BPNN is a multi-layer feedforward neural network, which is trained by the error back propagation algorithm, and it has strong nonlinear mapping ability and a wide range of applications. Considering the complex correlation of data in high-speed mobile scenario, BPNN is employed to estimate DFO in the proposed method.

Fig. 1 shows the structure of BPNN with L layers, which contains $L-2$ hidden layers. In Fig. 1, the input of the bth node of the lth layer can be expressed as

$$x_b^{(l)} = \boldsymbol{w}_{b,\boldsymbol{a}}^{(l)\mathrm{T}} \boldsymbol{I}_{\boldsymbol{a}} \tag{3}$$

where $\boldsymbol{a}$ represents a set of nodes in the $(L-1)$th layer connected to the node b. $\boldsymbol{w}_{b,\boldsymbol{a}}^{(l)}$ is a weight vector between the node b and each node in $\boldsymbol{a}$. $\boldsymbol{I}_{\boldsymbol{a}}$ is the input vector of the $(L-1)$th layer node.

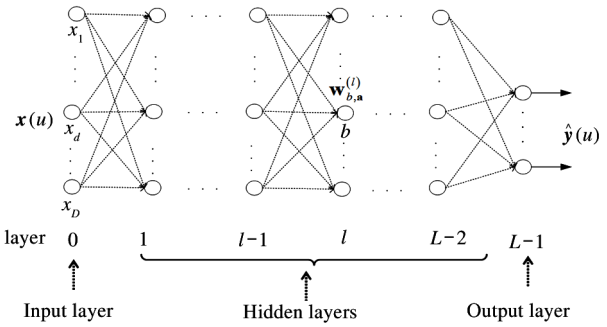

Fig. 1 The structure of BPNN

In BPNN, the output of the node is the value obtained by weighting all the inputs and then processing them through the transfer function, so the output of the node bth of the lth layer is

$$y_b^{(l)} = f(x_b^{(l)}) = f(\boldsymbol{w}_{b,\boldsymbol{a}}^{(l)\mathrm{T}} \boldsymbol{I}_{\boldsymbol{a}}) \tag{4}$$

where $f(\cdot)$ represents the transfer function, and different transfer functions can be selected according to the specific application. In the proposed method, the Tansig and Purelin transfer functions are respectively employed in the hidden layer and output layer, i. e.,

$$\begin{aligned} f_{\mathrm{Tansig}}(x) &= \frac{2}{1+e^{-2x}} - 1 \\ f_{\mathrm{Purelin}}(x) &= x \end{aligned} \tag{5}$$

Define $\boldsymbol{\theta}^{(l)}$ is the set of the weights and thresholds for the lth layer of BPNN, and $\boldsymbol{\theta}^{(l)} = \{\boldsymbol{w}^{(l)}, \boldsymbol{v}^{(l)}\}$, where $\boldsymbol{w}^{(l)}$ and $\boldsymbol{v}^{(l)}$ respectively represent the weight vector and threshold vector of the lth layer. $\boldsymbol{w}^{(l)} = [\boldsymbol{w}_{1,\boldsymbol{a}}^{(l)}, \cdots, \boldsymbol{w}_{Q_l,\boldsymbol{a}}^{(l)}]$ and $\boldsymbol{v}^{(l)} = [\boldsymbol{v}_{1,\boldsymbol{a}}^{(l)}, \cdots, \boldsymbol{v}_{Q_l,\boldsymbol{a}}^{(l)}]$, where Q_l is the number of the neurons of lth layer. Denote $\boldsymbol{\theta} = \{\boldsymbol{\theta}^{(l)}\}_{l=1}^{L-1}$, and $Loss_{\boldsymbol{\theta}}$ is the loss function, which is given as

$$Loss_{\boldsymbol{\theta}} = \frac{1}{UL_y} \sum_{u=0}^{U-1} \| \hat{\boldsymbol{y}}(u) - \boldsymbol{y}(u) \|_1 \tag{6}$$

where $\boldsymbol{y}(u)$ is the output of BPNN, and $\hat{\boldsymbol{y}}(u)$ is the estimation of $\boldsymbol{y}(u)$. L_y is the size of the vector $\boldsymbol{y}(u)$, and U is the number of the input data set. By minimizing $Loss_{\boldsymbol{\theta}}$ in and off-line training manner, one can obtain the optimal $\boldsymbol{\theta}$.

2.2 DL-based DFO estimation algorithm

The proposed method contains pre-training, training, and estimation stages, which can be seen from Fig. 2, where $\boldsymbol{\Gamma}_R(\cdot)$ represents the reshaping function given in Eq. (8). BPNN is firstly trained by an off-line manner at the pre-training and training stages. At the estimation stage, DFO will be estimated in real time by using little pilots. Moreover, the initial DFO estimation is also used as input to further improve the estimation accuracy.

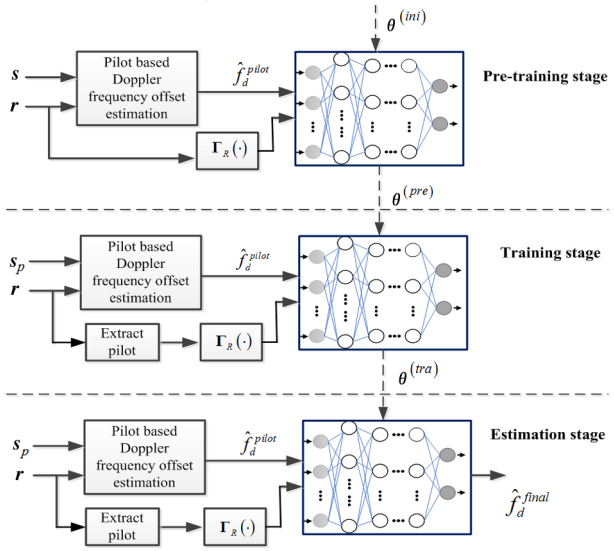

Fig. 2 The proposed algorithm

(1) Pre-training phase. To reduce the performance loss caused by the random initialization, the pre-training approach is firstly employed to obtain a desirable initialization, which is used as the initial parame-

ters of the training stage.

In pre-training stage, assume that the uth training sample set of BPNN is

$$\boldsymbol{X}_{\text{pre}}(u) = [R(1), R(2), \cdots, R(N_u), \hat{f}_d] \tag{7}$$

where $0 \leqslant u \leqslant U-1$, U is the number of the training sample sets. $R(k)$ represents the received signal at the kth subcarrier, which is obtained by IFFT of $r(m, n)$ given in Eq. (4) and includes pilot and information symbols. N_u is the number of the used subcarrier for one OFDMA symbol, which includes N_p pilot and $N_u - N_p$ information symbols. $\hat{f}_d$ is the estimated Doppler frequency offset by the algorithm given in Ref. [11] with information symbols known.

The input data must be reshaped because BPNN can only work in real domain. Assume that $\boldsymbol{\Gamma}_R(Z)$ is the input reshaping function, i. e.,

$$\boldsymbol{\Gamma}_R(Z) = [\Re\{Z\}, \Im\{Z\}] \tag{8}$$

where $\Re\{Z\}$ and $\Im\{Z\}$ are the operations of taking the real and imaginary parts of Z, respectively.

Then, the real input data of the BPNN in the pre-training stage are given as

$$\boldsymbol{X}_{\text{pre}}(u) = [\boldsymbol{\Gamma}_R(R(1)), \cdots, \boldsymbol{\Gamma}_R(R(N_u)), \hat{f}_d] \tag{9}$$

In the pre-training stage, the biases of the BPNN are initialized to be constants close to 0, and $\boldsymbol{\theta}^{(ini)}$ is denoted as the initial parameters of the BPNN[18]. Based on the initial parameters, the training sample set is employed to train BPNN. By minimizing $Loss(\boldsymbol{\theta})$ with the Levenberg-Marquardt (LM) algorithm, one can obtain the converged parameters of the BPNN $\boldsymbol{\theta}^{(\text{pre})}$.

(2) Training phase. Assume that $\boldsymbol{X}_{\text{tra}}(u)$ is the uth real training sample set in this stage, i. e.,

$$\boldsymbol{X}_{\text{tra}}(u) = [\boldsymbol{\Gamma}_R(R(1)), \cdots, \boldsymbol{\Gamma}_R(R(N_p)), \underbrace{0, \cdots, 0}_{N_u - N_p}, \hat{f}_d] \tag{10}$$

where $R(1), \cdots, R(N_p)$ are the received pilot, $\hat{f}_d$ is the estimated Doppler frequency offset by the algorithm given in Ref. [11] only with pilot.

In the training stage, the $\boldsymbol{\theta}^{(\text{pre})}$ obtained in the pre-training phase are used as initial parameters of the BPNN, and the training sample set is used to train the network. By minimizing $Loss(\boldsymbol{\theta})$ with the LM algorithm, one can obtain the final weights and thresholds $\boldsymbol{\theta}^{(\text{tra})}$.

In the training phase, the training samples are the received pilots and estimated DFO, where the DFO is estimated only by the pilots. However, training samples are the estimated DFO and received signal in the pre-training phase, where the DFO is estimated by the information and pilot symbols, which can improve the estimation accuracy. Moreover, the proposed DL-based estimator adopts $\hat{f}_d$ as part of the input such that the BPNN can further improve the performance.

(3) Estimation phase. The estimation stage is the process of DFO estimation in an online manner by using the network model obtained in the training stage. Moreover, the input data in the estimation stage has same structure as that in the training stage. By feeding the input data into the trained BPNN, one can obtain the DFO estimation.

3 Simulation results

3.1 MSE performance

To evaluate the performance of the proposed method, a 5G-NR for HSR scenario is considered[24-26]. The simulation parameters are given as follows: the length of one slot is 250 μs, and each slot contains 14 OFDMA symbols. The length of FFT is 1024, and the carrier frequency is 30 GHz. The pilot uses the centralized placement. The cyclic prefix (CP) length is 128. The sub-carrier spacing is 60 kHz, and the vehicle speed is 500 km/h. The single path Ricean channel model is considered, and the Ricean factors are 5 and 10. In comparison with the proposed method, the previous work in Ref. [15], the pilot segment based DFO estimation method in Ref. [11], and the pilot based maximum likelihood estimation (ML) method in Ref. [13] are also simulated.

Fig. 3 gives the mean squared error (MSE) performances of the DL-based DFO estimation method with different training methods and training parameters. In Fig. 3, the DL-based without pre-training and only using

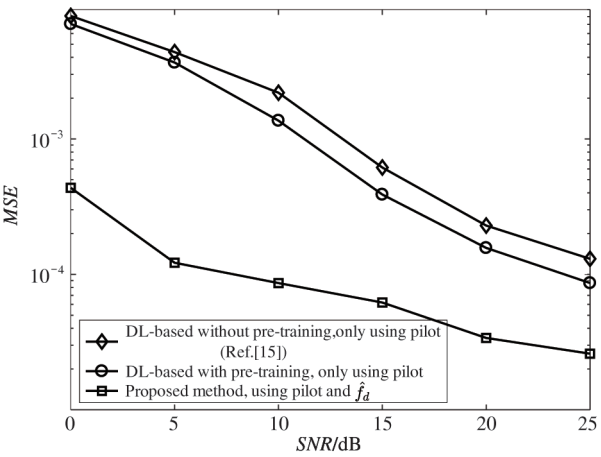

Fig. 3 MSE performances of the DL-based DFO estimation method with different training methods and training parameters (Ricean factor is 10)

pilot symbols is the previous work given in Ref. [15]. In the simulation, the number of used pilot is 72 for DL-based without pre-training, and the number of used pilot for pre-training and training are 72 and 16 respectively for both DL-based with pre-training and proposed method. Compared with the DL-based without pre-training given in Ref. [15], the DL-based with pre-training method has a better performance due to its using pre-training. However, the proposed method has a best performance due to employing the pre-training and initial estimation $\hat{f}_d$.

Fig. 4 shows the MSE performance under the different numbers of training sample sets for the proposed method. In the simulation, the number of pilots N_p in each sample set is the same, and $N_p = 16$. In Fig. 4, one can see that the accuracy of DFO estimation is improved as the number of sample sets U increases, which indicates that the larger training sample sets can improve the learning efficiency of the neural network, but it will also increase the complexity of offline training. Therefore, the choice of the number of training sample sets should be a compromise between performance and computational complexity in practice.

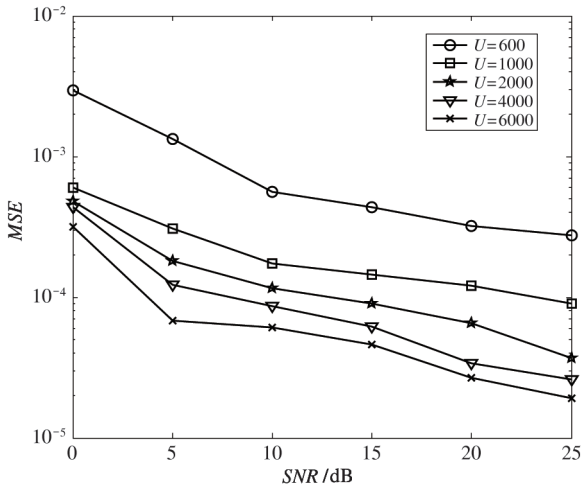

Fig. 4 MSE performance under different numbers of training sample sets for the proposed method (Rican factor is 10)

Fig. 5 shows the MSE performance of the DFO estimation by the network trained under different signal-to-noise ratios (SNRs) conditions for the proposed method. When the SNR is lower than 12 dB, the performance of proposed method with the network trained under the fixed SNR of 10 dB is better than that of the network trained under the 20 dB, and when the SNR is greater than 12 dB, the performance of the network trained under the 20 dB is better. When training the network with varying SNRs, the proposed method can maintain good performance regardless of whether SNR is low or high. Therefore, when DFO estimation is performed, in order to maintain better estimation performance, a suitable neural network can be selected according to different SNRs for estimation.

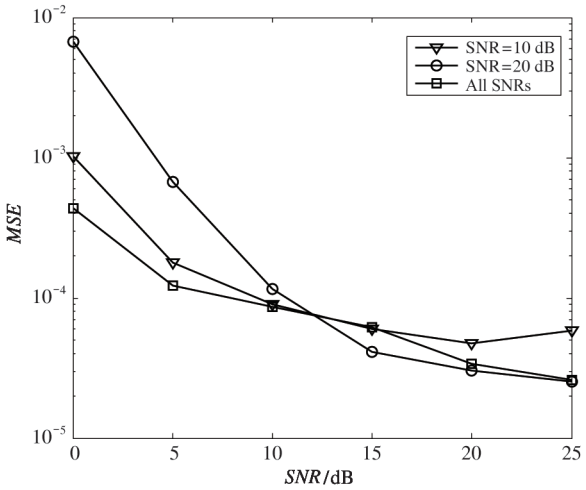

Fig. 5 MSE performance of proposed method by training under different SNRs (Rican factor is 10)

Fig. 6 shows the MSE performances of the different DFO estimation methods with the different Ricean factors. In simulation, $U = 4000$ and $N_p = 32$ for the proposed method, and $N_p = 1024$ and the number of the segments is 2 both for the schemes in Ref. [11] and Ref. [13]. From Fig. 6, the proposed method can obtain the best performance but only using a little pilot, while the algorithms in Ref. [11] and Ref. [13] are limited by the number of pilot segments, so they have a poor estimation performance. Moreover, the performance of all methods will be improved as Ricean factor increases.

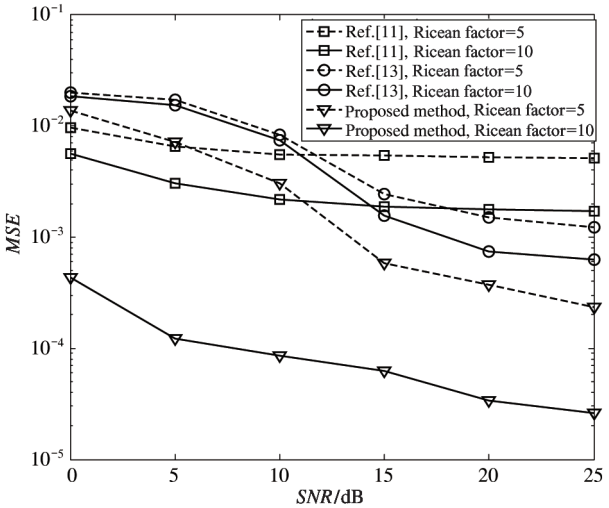

Fig. 6 MSE performances of different DFO estimation methods with different Ricean factors

3.2 Complexity analysis

The section will give the comparison of the computational complexity of different Doppler frequency offset estimation methods. The number of floating point operations (FLOPs) is considered as the criterion of complexity. Ref. [11] and Ref. [13] need $4N+2$ and $N+3N_{cp}+11T$ FLOPs respectively, and the proposed method needs $2U\sum_{l=1}^{L-1}Q_{l-1}Q_l$ FLOPs in off-line stage and $\sum_{l=1}^{L-1}Q_{l-1}Q_l$ FLOPs in online stage, where T is the number of searches and L is the number of the BPNN layers, Q_l is the number of neuron nodes of the lth layer.

Assume that $L=3$ and $T=100$, the number of neurons in the two hidden layers is 20 and 50 respectively. In the case, the complexity of the proposed method in the off-line stage is larger than those of the algorithms in Ref. [11] and Ref. [13], while its complexity in online stage is close to those of the algorithms in Ref. [11] and Ref. [13]. However, the proposed method only needs to train the neural network once in an off-line manner for the same wireless environments, and the network can be used to obtain the DFO estimation in an on-line manner. Moreover, the estimation performance of the proposed method is best, which can be seen from Fig. 6.

4 Conclusions

A DL-based DFO estimation method is proposed for 5G-NR HSR scenario. After training the network in an off-line manner, the proposed method only uses little pilots to obtain the high-precision DFO estimation in an online manner, which has low computational complexity. The proposed method is not only suitable for 5G-NR HSR scenarios, but also can be employed to estimate the DFO in existing and future high-speed mobile communication scenarios.

References

[1] HU Y, LI H, CHANG Z, et al. Scheduling strategy for multimedia heterogeneous high-speed train networks[J]. *IEEE Transactions on Vehicular Technology*, 2017, 66(4): 3265-3279

[2] SUN N, ZHAO Y, SUN L, et al. Distributed and dynamic resource management for wireless service delivery to high-speed trains[J]. *IEEE Access*, 2017, 5: 620-632

[3] GHAZZAI H, BOUCHOUCHA T, ALSHAROA A, et al. Transmit power minimization and base station planning for high-speed trains with multiple moving relays in OFDMA systems[J]. *IEEE Transactions on Vehicular Technology*, 2017, 66(1): 175-187

[4] GUAN K, LI G K, KÜRNER T, et al. On millimeter wave and THz mobile radio channel for smart rail mobility [J]. *IEEE Transactions on Vehicular Technology*, 2017, 66(7): 5658-5674

[5] AI B, GUAN L, RUPP M, et al. Future railway services-oriented mobile communications network[J]. *IEEE Communications Magazine*, 2015, 53(10): 78-85

[6] LEVANEN T, TALVITIE J, WICHMANY R, et al. Location-aware 5G communications and Doppler compensation for high-speed train networks[C]// Proceedings of 2017 European Conference on Networks and Communications (EuCNC), Oulu, Finland, 2017: 1-6

[7] SEUNG N C, LLGYU K. Performance improvement of MHN-enhanced uplink with frequency offset compensation [C]// Proceedings of 2017 9th International Conference on Ubiquitous and Future Networks (ICUFN), Milan, Italy, 2017: 788-790

[8] FAN D, ZHONG Z D, WANG G P, et al. Doppler shift estimation for high-speed railway wireless communication systems with large-scale linear antennas[C]// Proceedings of 2015 International Workshop on High Mobility Wireless Communications (HMWC), Xi'an, China, 2015: 1-5

[9] LI J X, ZHAO Y P. Radio environment map-based cognitive Doppler spread compensation algorithms for high-speed rail broadband mobile communications[J]. *EURASIP Journal on Wireless Communications and Network*, 2012, 263:1-18

[10] HOU Z W, ZHOU Y Q, SHI J L, et al. Radio environment map-aided Doppler shift estimation in LTE railway [J]. *IEEE Transactions on Vehicular Technology*, 2017, 66(5):4462-4467

[11] SHUO S. Research and Implementation of Synchronization Algorithm in Multipath Fast Time-varying Environment[D]. Xi'an: School of Telecommunications Engineering, Xidian University, 2017 (In Chinese)

[12] HUI B, KIM J, CHUNG H S, et al. Efficient Doppler mitigation for high-speed rail communications[C]// Proceedings of the 18th International Conference on Advanced Communication Technology, PyeongChang, Korea, 2017: 1-6

[13] ZHANG C, WANG G P, HE R S, et al. A Doppler shift estimator for millimeter-wave communication systems on high-speed railways[C]//Proceedings of 2018 IEEE/CIC International Conference on Communications in China(ICCC), Beijing, China, 2018: 227-231

[14] MAO Q, HU F, HAO Q. Deep learning for intelligent wireless networks: a comprehensive survey[J]. *IEEE Communications Surveys and Tutorials*, 2018, 20(4): 2595-2621

[15] WANG Z H, YANG L H, CHENG L. BP neural network based Doppler frequency offset estimation method for 5G high-speed mobile system[J]. *Telecommunications Science*, 2020, 4: 83-90

[16] MA X, YE H, LI Y. Learning assisted estimation for time-varying channels[C]//Proceedings of 2018 15th International Symposium on Wireless Communication Systems (ISWCS), Lisbon, Portugal, 2018: 1-5

[17] BAI Q, WANG J, ZHANG Y, et al. Deep learning-

based channel estimation algorithm over time selective fading channels[J]. *IEEE Transactions on Cognitive Communications and Networking*, 2020, 6(1): 125-134

[18] YANG Y W, GAO F F, MA X L. Deep learning-based channel estimation for doubly selective fading channels [J]. *IEEE Access*, 2019, 7: 36579-36589

[19] KANG J, CHUM C, KIM I. Deep learning based channel estimation for MIMO systems with received SNR feedback [J]. *IEEE Access*, 2020, 8: 121162-121181

[20] ABRISHAMKAR F, IRVINE J. Comparison of current solutions for the provision of voice services to passengers on high speed train[C]// Proceedings of IEEE Vehicular Technology Conference, Boston, USA, 2000: 2068-2075

[21] GOLLER M. Application of GSM in high speed trains: measurements and simulations[J]. *IEEE Colloquium on Radio Communications in Transportation*, 1995, (5): 1-7

[22] 3GPP. TSG-RAN4-37 Initial ideal simulation results for different high speed propagation scenarios[S]. Seoul, Korea: 3GPP, 2005

[23] YANG L H, REN G L, QIU Z L. A novel Doppler frequency offset estimation method for DVB-T system in HST environment[J]. *IEEE Transactions on Broadcasting*, 2012, 58 (1): 139-143

[24] SONG H, FANG X M, FANG Y G, et al. Millimeter-wave network architectures for future high-speed railway communications: challenges and solutions [J]. *IEEE Wireless Communications*, 2016, 23: 114-122

[25] 3GPP, TR 38.900 v14.3.1 3rd generation partnership project; technical specification group radio access network; study on channel model for frequency spectrum above 6 GHz (Release 14)[S]. Valbonne, France: 3GPP, 2017

[26] 3GPP, TR 38.912 v14.1.0 3rd generation partnership project; technical specification group radio access network; study on new radio (NR) access technology (Release 14)[S]. Valbonne, France: 3GPP, 2017

YANG Lihua, born in 1984. She received her Ph. D degree in the communication and information systems at Xidian University in 2013. She also received her B. S. degree at Xi'an University of Science and Technology in 2007 and her M. S. degree at Xidian University in 2008. Her research interests include the key technologies of the physical layer in the mobile wireless communications and channel model.